Heliyon 9 (2023) e18482

Contents lists available at ScienceDirect

Heliyon

journal homepage: www.cell.com/heliyon

Research article

Stem cell-derived brain organoids for controlled studies of transcranial neuromodulation

Jan Kubanek [b,*], Matthew Wilson [b], Richard D. Rabbitt [b], Celeste J. Armstrong [a], Alexander J. Farley [b], H. M. Arif Ullah [a], Alex Shcheglovitov [a,b]

[a] University of Utah, Department of Neurobiology, 20 South 2030 East, Salt Lake City, UT 84112, United States of America
[b] University of Utah, Department of Biomedical Engineering, 36 South Wasatch Dr, Salt Lake City, UT 84112, United States of America

ARTICLE INFO

Keywords:
Intracranial
Recordings
Skull
Focused ultrasound
Rhythms
Durable

ABSTRACT

Transcranial neuromodulation methods have the potential to diagnose and treat brain disorders at their neural source in a personalized manner. However, it has been difficult to investigate the direct effects of transcranial neuromodulation on neurons in human brain tissue. Here, we show that human brain organoids provide a detailed and artifact-free window into neuromodulation-evoked electrophysiological effects. We derived human cortical organoids from induced pluripotent stem cells and implanted 32-channel electrode arrays. Each organoid was positioned in the center of the human skull and subjected to low-intensity transcranial focused ultrasound. We found that ultrasonic stimuli modulated network activity in the gamma and delta ranges of the frequency spectrum. The effects on the neural networks were a function of the ultrasound stimulation frequency. High gamma activity remained elevated for at least 20 minutes following stimulation offset. This approach is expected to provide controlled studies of the effects of ultrasound and other transcranial neuromodulation modalities on human brain tissue.

1. Introduction

One in three patients with a neurological or mental disorder does not respond to drugs or other forms of treatment [6,1,25,39,64,14,15,17,26,38]. Neuromodulation provides these patients with new treatment options, promising to treat brain disorders at their neural sources [33,47,62,4,32,11,53].

Nonetheless, current neuromodulation approaches have significant limitations, which make them applicable only to certain indications and patients. In particular, invasive approaches such as deep brain stimulation have been used for treatment-resistant movement disorders, such as Parkinson's disease [33], for which there are established implantation targets. On the other hand, the more flexible, transcranial neuromodulation approaches, including electrical [43,36,22], magnetic [21,58], electromagnetic [40,8], or ultrasonic (see [42,31,3]) neuromodulation, currently suffer from limited effectiveness. This limitation is, at least partially, due to our incomplete understanding of the neuromodulatory effects on the neural tissue inside the skull.

To address this issue, we developed a model that can elucidate the effects of transcranial neuromodulation at a detailed, circuit level. Specifically, we investigated the effects of transcranial focused ultrasound on neural activity of human stem-cell derived

* Corresponding author.
E-mail address: jan.kubanek@utah.edu (J. Kubanek).

https://doi.org/10.1016/j.heliyon.2023.e18482
Received 24 July 2022; Received in revised form 17 July 2023; Accepted 19 July 2023

Available online 26 July 2023

telenecephalic organoids [29,61]. The organoids model key three-dimensional electrical and mechanical ties between cells [24,12,9]. Compared with recordings from live animals or humans, the organoids are free from peripheral artifacts that commonly arise during neuromodulation, such as auditory or tactile artifacts [23,52,5,37]. The inclusion of the human skull takes into account critical geometrical constraints and field aberration properties of transcranial neuromodulation [50].

2. Materials and methods

2.1. Human brain organoids

We have developed a system that enables electrophysiological recordings from human brain organoids. The organoids were induced using single induced pluripotent stem cell (iPSC)-derived neural rosettes [61]. We specifically used a dual SMAD inhibition protocol (see [7]) to efficiently differentiate iPSCs into dorsal anterior forebrain neural progenitors that express Pax6 and FoxG1 and that are organized into stereotypical structures called neural rosettes [61]. Under a stereoscope, the single rosettes were isolated for growth in suspension culture for another four to five months. The single-rosette cortical organoids (SRCOs) grow large in suspension culture, reaching 4–5 mm in diameter by four months (**Fig. 1**A), and maintain a single ventricle-like internal lumen throughout the differentiation [61]. Immunohistochemistry revealed (see [61]) that the SRCOs consisted of Pax6-expressing cortical neural progenitors, GFAP-expressing astrocytes, and different subtypes of cortical excitatory neurons expressing Satb2 (upper layer neurons) and Ctip2 and Tbr1 (lower layer neurons). The SRCOs also contain inhibitory neurons expressing GABA that are properly organized around the internal lumen [61]. The single-rosette method reduces the experimental variability associated with the presence of multiple internal lumens and corresponding germinal zones per organoid, which has been reported in previous studies, and provided us with a predictably organized human cortical tissue suitable for electrophysiological recordings [61].

2.2. Apparatus

To allow efficient implantation of organoids with multi-electrode array probes for monitoring electrical activity, we manufactured a recording chamber, in which a C-shaped rubber tubing was glued to the surface of a 6 cm Petri dish (**Fig. 1**A-B). This feature has helped to keep organoids in place during the implantation and recording. We used one organoid per dish. For implantation, an organoid was immersed in Neurobasal medium (ThermoFisher). An ultrasound transducer (H-115, Sonic Concepts) was placed at the bottom of a tank filled with deionized and degassed water (**Fig. 1**C). A degassed human *ex-vivo* skull was positioned, upside down, over the transducer and secured to the tank (**Fig. 1**D). The Petri dish containing each organoid was placed on a plastic stand with 4 x 4 cm opening for the ultrasound beam. The stand was 6 cm above the transducer face and thus coincided with the focal distance of the ultrasonic transducer. Before each experiment, we used a hydrophone (HGL-200, Onda) to validate the focus of the ultrasound along the lateral x and y coordinates. To do so, we gradually moved the hydrophone with a 3D manipulator until detecting the peak of the field. We then placed the dish such that the hydrophone tip pointed at the organoid. In addition to the positioning, the hydrophone was used to maintain the same stimulation amplitude (0.65 MPa) across experiments.

2.3. Experimental timeline

We first recorded 5-minute baseline during which no ultrasound was applied. Following this period, ultrasound was delivered into the organoid for 15 minutes. This period was followed by a 20-minute off period during which there was no ultrasound.

2.4. Ultrasonic stimuli

Besides the ultrasound frequency (270 kHz or 885 kHz), all other parameters were fixed. The pressure amplitude was 0.65 MPa at target in all cases. The amplitude was chosen to lie safely below the FDA 510(k) Track 3 guidelines for safe ultrasound exposure [16]. The ultrasound was pulsed at 60 Hz pulse repetition frequency. This frequency was chosen to coincide with the frequency of line noise, which was filtered out using a notch filter. The ultrasound was pulsed at 5% duty to stay below the FDA 510(k) I_{SPTA} average intensity level (see [16]) and therefore to prevent heating. For this value of duty cycle, $I_{SPTA} = 682$ mW/cm^2, given the acoustic impedance of 1.55 MRayl. The stimuli were generated by a function generator (KeySight) and amplified using a broadband (250 kHz to 30 MHz) amplifier (A150, ENI). Sham stimulation was delivered 20 mm off of each organoid (dashed outline in **Fig. 1**B). The sham was performed at the higher frequency as that frequency showed the more prominent effects of stimulation.

2.5. Electrophysiological recordings

We implanted 32-electrode recording arrays (A1x32-6mm-100-177, NeuroNexus) into each organoid 6-months post induction (5-month post-fusion). The arrays were inserted manually into the tissue until only the last reference electrode was outside. The connector (Omnetics) of each array was attached to the scalable dish (**Fig. 1**A) and connected to a head stage and a stimulation/recording controller (RHS2000, Intan Technologies). Signals were low-pass filtered at 7 kHz and sampled at 30 kHz to avoid aliasing. For maintenance of a stable 37 °C recording environment, a precision thermistor (3950 NTC, Dikavs) was permanently attached to each bath. The thermistor reading was calibrated to correspond to 37 °C inside the bath. The temperature was maintained at 37 °C using an Arduino control system attached to Titanium Aquarium Heater (H2Pro). Data were collected on an air table inside a Faraday cage to

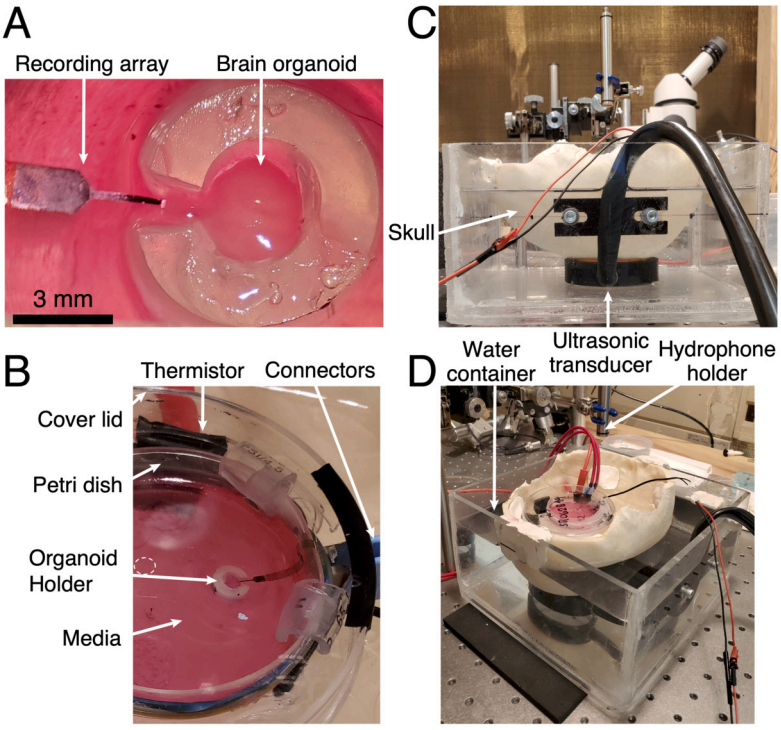

Fig. 1. Recordings from human brain organoids during transcranial neuromodulation. A) Human cortical organoids were derived from induced pluripotent stem cells (H9, 6 months old), and implanted with a linear 32-channel electrode array. B) The organoids were maintained in a Petri dish and held in place using a C-shaped plastic boundary. The connectors of the recording arrays were secured to the dish. A thermistor measured the temperature of the nourishing media. The white dashed oval outlines the off-target stimulation location. C) The dish with each organoid was placed in the geometric center of a human skull. An immersible ultrasound transducer was positioned beneath the skull. D) The setup was housed in a water container to ensure reliable propagation of the ultrasound into the target. The dish with the organoid was placed into the location of the maximal ultrasound intensity, 6 cm above the transducer face. The target intensity was validated using a hydrophone. The stimulation and recordings were performed on an air table inside a Faraday cage. A grounding cable (thick red) was immersed in the water to provide the reference and the ground for the recordings.

curb the impact of external vibrations or electromagnetic noise. The recorded data were visually inspected for artifacts. Of the 192 channels in 6 organoids, 1 channel was excluded in the 270 kHz dataset and 5 channels in the 885 kHz dataset. The 60 Hz power line was filtered out using a notch filter. Data analyses were performed using custom Matlab scripts. Spectral analysis was performed using the Fast Fourier Transform (periodogram command in Matlab). The analyzed frequency ranges comprised delta (1–4 Hz), theta (4–7 Hz), alpha (8–12 Hz), beta (13–30 Hz), gamma (30–50 Hz), and high gamma (70–110 Hz).

2.6. Optical measurements

Displacement measurements were obtained using an MV-H-S laser vibrometer (OmniSensing Photonics, Columbia, MD). The stimulation was performed in the same manner as during the electrophysiological recordings with the exception that organoids were replaced with the transparent Matrigel (Corning Life Sciences, USA). The optical transparency of the Matrigel enabled us to measure the displacements optically, at high spatial and temporal resolution. The vibrometer recorded displacements at a sampling rate of 1.25 MHz, high enough for the 270 kHz ultrasound. The vibrometer was placed 80 mm from the electrode array embedded in the Matrigel. An IR detector card was used to validate the laser's targeting. Ultrasound was applied for 3 seconds at 0.6 MPa with a frequency of 270 kHz, pulsed at 60 Hz and 5% duty cycle. Responses were recorded using the OmniSensing Photonics software.

3. Results

In a recent study, we generated telencephalic organoids from isolated neural rosettes and demonstrated that 6-month-old organoids develop spontaneous network activity and oscillations that are abolished by the application of a voltage-gated sodium channel blocker TTX [61]. Here, we tested whether these organoids could be used for studying the effects of ultrasound on human neural networks. We recorded electrophysiological responses from the organoids using implanted multi-electrode arrays, while the organoids were subjected to ultrasound focused through the intact human skull (**Fig. 1**).

The transducer operated at two distinct frequencies (270 kHz fundamental and a 885 kHz harmonic), which enabled us to test the responses of the organoids to low and high frequencies of neuromodulatory ultrasound [49]. We evaluated the responses of the organoids to 15-minute stimulation protocol. We hypothesized that sustained ultrasonic modulation elicits durable changes in neural

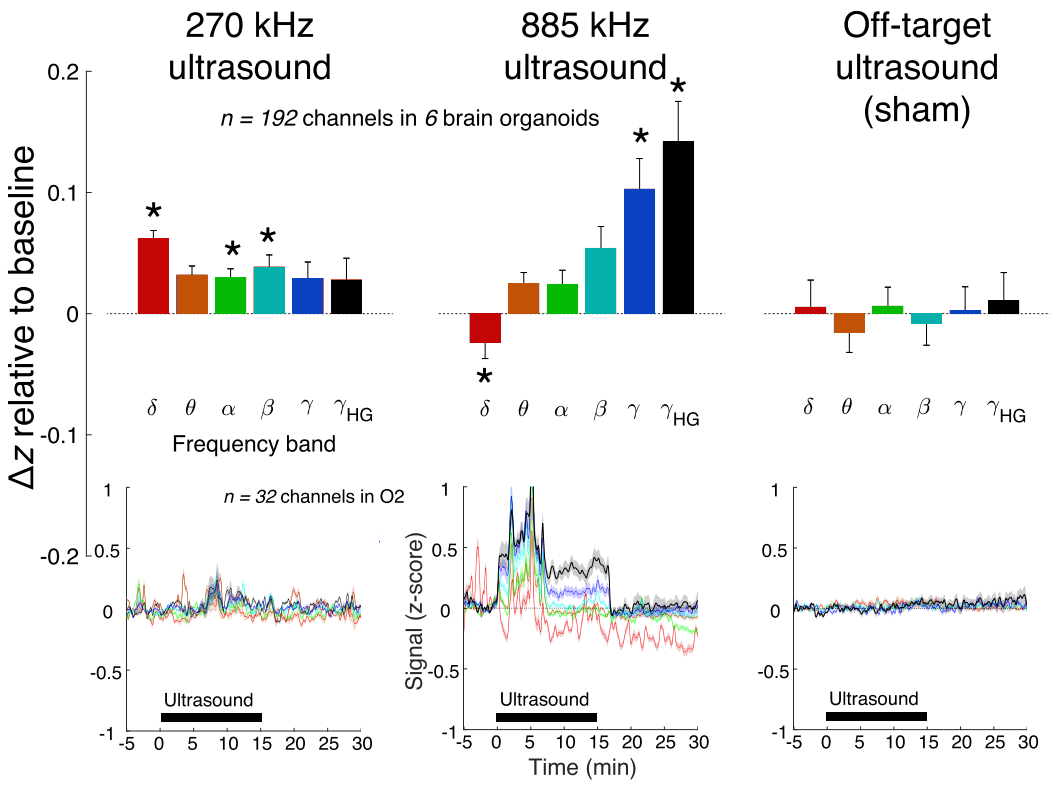

Fig. 2. Electrophysiological effects. Mean±s.e.m. changes of z-scored neural signals within specific frequency bands (see inset and Materials and Methods) during the 15 minute stimulation relative to a 5 min pre-stimulation baseline. These epochs are highlighted in single-organoid (organoid O2) time course examples on the bottom. The effects are provided separately for the low-frequency (left plot) and the high-frequency (middle plot) ultrasound stimuli. Sham stimulation (right plot) delivered the high-frequency ultrasound 20 mm off-target. Stars denote effects significant at $p < \frac{0.05}{6}$ (two-sided t-test, Bonferroni correction for multiple comparisons).

activity, and these changes are specific to particular neural rhythms [35,60,19]. The ultrasound pressure was set to 0.65 MPa at the organoid location for both frequencies, and was pulsed at 5% duty and 60 Hz pulse-repetition frequency to prevent heating during the stimulation (see Materials and Methods for additional reasons).

We quantified the responses of the brain organoids in standard frequency bands ranging from delta to high gamma [61]. **Fig. 2** shows the changes of z-scored activity within each band during the 15-minute stimulation relative to a 5 minute baseline prior to the stimulation. The ultrasound stimulation modulated the activity in specific frequency bands, and the effects depended on the frequency of the applied ultrasound (**Fig. 2**). A two-way ANOVA with factors of ultrasound frequency and signal band detected a significant effect of ultrasound frequency ($F(1,2256) = 6.5$, $p = 0.011$), signal band ($F(5,2256) = 9.3$, $p = 9.4 \times 10^{-9}$) as well as a significant interaction between these two factors ($F(5,2256) = 8.9$, $p = 2 \times 10^{-8}$). Post-hoc t-tests specifically revealed a significant change ($p < \frac{0.05}{6}$; Bonferroni correction) in the high-gamma ($t(186) = 4.48$, $p = 1.3 \times 10^{-5}$), gamma ($t(186) = 3.91$, $p = 0.00013$), and delta ($t(186) = -3.09$, $p = 0.0023$) bands for the high-frequency ultrasound stimulus, and beta ($t(190) = 2.73$, $p = 0.007$), alpha ($t(190) = 3.12$, $p = 0.0021$), and delta ($t(190) = 6.60$, $p = 4 \times 10^{-10}$) bands for the low-frequency ultrasound stimulus. There were no significant effects during a sham condition, in which the high-frequency stimulus was aimed 20 mm off of each organoid (**Fig. 2**, right). These results suggest that ultrasound modulates specific neural rhythms in stimulation frequency-dependent manner, and that the effects are specific to the ultrasound focus.

We next investigated the variability of ultrasound-induced responses from organoid-to-organoid by including the number of each organoid as an additional factor in the ANOVA. The 3-way ANOVA indeed revealed a significant effect ($F(5,2196) = 46.0$, $p = 2.9 \times 10^{-45}$). We inspected this effect in detail, by plotting the strongest effect (high gamma modulation for the 885 kHz stimulus; **Fig. 2**) separately for the individual organoids. **Fig. 3** revealed that 50% (3 of 6) organoids showed significant modulation ($p < \frac{0.05}{6}$; two-sided t-test, Bonferroni correction for multiple comparisons). This outcome serves as an additional control for potential artifacts that could be associated with the stimulation, but also indicates that there is organoid-to-organoid variability in the ultrasound-induced responses.

We investigated the temporal dynamics of the effects for the organoids responsive to the ultrasonic stimulation (**Fig. 3**). **Fig. 4** confirms the effects of **Fig. 2** that the high-frequency stimulus substantially modulated activity in the gamma, high gamma, and delta frequency bands. Notably, the changes in the high gamma and delta activity outlive the stimulus duration. Indeed, in the window from 15-30 min, both the high gamma ($t(95) = 3.85$, $p = 0.00021$, two-sided t-test) and the delta ($t(95) = -6.80$, $p = 9.4 \times 10^{-10}$) effects remain significant. Therefore, ultrasonic stimulation can exert sustained, durable effects on high gamma and delta activity.

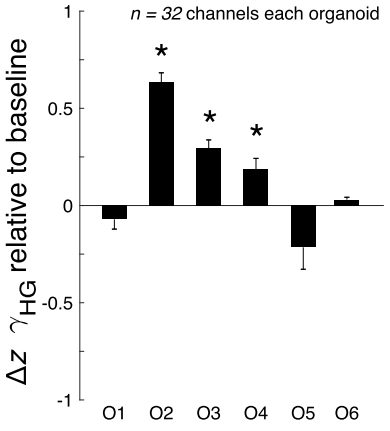

Fig. 3. Effects for individual organoids. Same format as in **Fig. 2** specifically for high gamma activity at 885 kHz, separately for each organoid. Stars denote effects significant at $p < \frac{0.05}{6}$ (two-sided t-test, Bonferroni correction for multiple comparisons). The organoid-to-organoid variability was most apparent in the high gamma range.

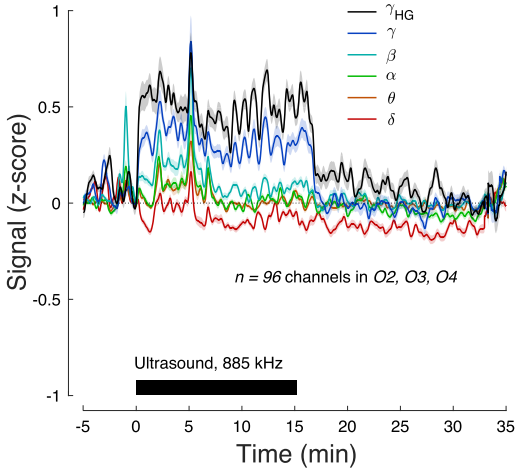

Fig. 4. Effect dynamics. Mean±s.e.m. activity within the individual bands as a function of time for the three responsive organoids (**Fig. 3**). The activity is aligned to the ultrasound onset (time 0). The activity in each band was computed in 0.5 s time windows, 0.25 s overlap. The traces were smoothed with a 10 s zero-lag averaging filter.

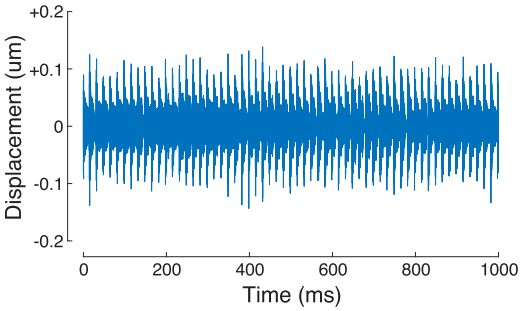

Fig. 5. Measurements of electrode displacements in response to ultrasonic stimulation. Typical time course of the displacement of the electrode array measured using an ultrafast laser vibrometer in response to the 270 kHz stimulation protocol. The stimulation was performed in the same manner as during the electrophysiological recordings with the exception that the organoids were replaced with the transparent Matrigel. The optical transparency of the Matrigel enabled us to measure the displacements optically, with high spatial and temporal precision.

Finally, we used an ultrafast laser vibrometer (see Materials and Methods) to assess the degree of displacement of the recording electrode in response to the sonication (**Fig. 5**). The optical measurements had a sampling rate of 1.25 MHz, which was high enough to assess the displacements during the 270 kHz ultrasound. Across 180 pulses of ultrasound, delivered in the same manner as

during the stimulation, we detected a mean±s.d. displacement of 113±46 nm and 114±49 nm for the positive and negative peaks, respectively.

4. Discussion

We developed a method that enables to study the responses of human brain tissue to transcranial neuromodulation. The approach records electrophysiological activity from ensembles of neurons within three-dimensional human cortical organoids. We combined volumetric recordings from the brain organoids (see [34,57]) with geometric constraints of the human skull, which presents a critical barrier for studies of transcranial neuromodulation [50].

The organoid-based approach has three notable strengths. First, neuromodulation is known to act on neuronal tissues volumetrically. Compared with single cells or two-dimensional cultures, the organoids model these three-dimensional interactions. Second, approaches such as ultrasonic neuromodulation induce mechanical effects on the target neural tissue [42,31,3]. The organoids incorporate three-dimensional mechanical and elastic ties of cells with their neighbors. And third, neuromodulation in intact organism often invokes peripheral artifacts, including auditory, tactile, and other artifacts [23,52,5,37]. Because the organoids do not possess sensory organs, there are no auditory, tactile, or other peripheral confounds.

This article provides initial examples on how organoid-based methods can begin to answer outstanding questions regarding electrophysiological effects of neuromodulation. Specifically, in the field of ultrasonic neuromodulation, it has been unclear whether lower (see [30,28,63,20,49]) or higher (see [41,31]) ultrasound frequencies stimulate neurons more effectively. We found that activity in the delta band can show diverging effects depending on the frequency—an increase at 270 kHz yet a decrease at 885 kHz (**Fig. 2**). Moreover, we found that activity in the gamma and high gamma bands was effectively only induced at 885 kHz (**Fig. 2**). Therefore, ultrasound stimulation frequency governs which rhythms are modulated and how. Because high gamma activity correlates strongly with multi-unit activity [44], our data suggest that high ultrasound frequencies are more potent in eliciting multi-unit discharge.

We found that the high gamma and delta effects outlived the stimulus offset (**Fig. 4**), suggesting sustained neuromodulation. The effects were observed for up to 20 min following the stimulus offset—the full duration of our recordings. Indeed, sustained effects of ultrasonic stimulation have been observed by multiple groups and multiple animal models [59,10,45,18,60,27], including in humans [2,51]. The organoid-based approach offers a new way to study these durable effects at a detailed electrophysiological level. Moreover, pharmacological and genetic manipulations of the organoids will be able provide future insights into the neuroplastic effects at the level of individual molecules and ion channels.

In this study, the ultrasound was applied through the intact skull from a distance of 6 cm away from each organoid. This serves to eliminate potential electrical confounds in the recordings. There are four additional lines of evidence that the reported effects are physiological and not artifactual. First, high gamma and delta effects outlasted the stimulation (**Fig. 4**). Because no ultrasound was applied to the organoids during that time, these effects are artifact-free. Second, no effects were observed during off-target stimulation (**Fig. 2**), which applied to the ultrasonic transducer the same electric field as during the verum, on-target stimulation. Third, there was a dissociation of the effects through the stimulation frequency (**Fig. 2**). Fourth, effects were observed only in a subset organoids, *ceteris paribus* (**Fig. 3**).

The finding that high gamma and delta effects outlasted the stimulation (**Fig. 4**) also controls for the possibility of the electrodes being vibrated by the ultrasound. No ultrasound was applied to the organoids during that time, and thus any effects are vibration-artifact-free. Effects during the stimulation could be affected by a vibration of the recording electrode, but there are two lines of evidence against that possibility. First, the measured displacements were on the order of 0.1 um (**Fig. 5**)—small with respect to neuronal size. Second, we pulsed the ultrasound at 60 Hz, and filtered the signals out at 60 Hz. Therefore, radiation forces associated with the ultrasound were filtered out.

The inclusion of the skull is key for studies of ultrasonic neuromodulation that are to be applicable to the human brain. The skull provides a critical set of constraints on the parameters (frequency, amplitude, waveform) of the ultrasound that can be used for transcranial neuromodulation. This way, the neuromodulatory effects observed for the parameters tested in this study are applicable to the system of the human head and brain.

The study has certain caveats. First, the organoid dishes were exposed to air outside of the incubator. The associated changes in CO2 levels could lead to changes in the acidity of the media. For this reason, we limited our recording window to 35 minutes (about 45 minutes total including setup). Second, although we used a single-rosette induction approach, which aims to reduce anatomical variability across organoids [61], we observed functional variability [55]. As a consequence, we found that only 50% of the organoids showed significant responses to ultrasound (**Fig. 3**). The organoid-to-organoid variability in the responses warrant future systematic studies on the time point at which organoids exhibit mature activity and responses to neuromodulation. Currently, this window is believed to lie between 6-12 months [48,34], though may depend on the specific induction method and the nourishing media. And third, although the effects of ultrasound were observed for around 20 minutes, the effects eventually vanished. Future studies should test a broader set of parameters (duration, fundamental and pulse repetition frequency, duty cycle) to induce more durable effects, which are key for ultimate treatments of brain disorders.

The human brain organoids provide a unique opportunity to study the effects of neuromodulation at a detailed level and as a function of specific neural circuits. For example, organoids that model complete neural networks, such as cortico-striato-thalamic networks, have been developed [54,46]. Moreover, it is possible to label each cell type and thus obtain a cell-specific information on neuronal activation by ultrasound [13]. Furthermore, the organoids are also amenable to pharmacological and genetic manipulations to provide further insights into neuromodulation effects on individual molecules and ion channels [56].

In summary, we have presented a method that provides electrophysiological recordings from human brain tissue during transcranial neuromodulation. The method models three-dimensional electrical and mechanical ties between cells, and has the capability to model complete neural circuits. Moreover, the method is free of auditory, tactile, or other peripheral artifacts that can be difficult to control for in animal models and humans. The method is expected to lead to protocols that maximize transient or sustained neuromodulation effects in specific neural circuits in humans. This has the potential to boost the effectiveness of emerging neuromodulation approaches and thus provide treatment options for the large number of treatment-resistant patients.

CRediT authorship contribution statement

J.K. and O.S. conceived and designed the experiments. J.K., M.W., and R.B. performed the experiments. J.K. and M.W. analyzed and interpreted the data. C.A. and A.U. contributed reagents, materials, and analysis tools. J.K. and O.S. wrote the paper.

Declaration of competing interest

The authors declare that they have no known competing financial interests or personal relationships that could have appeared to influence the work reported in this paper.

Acknowledgements

This work was supported by the NIH grants R00NS100986, R01NS123849, and by the Focused Ultrasound Foundation (Charles Steger Global Fellowship). We thank Karla Tapia and Lelah Alhemrani for assistance. The authors declare no competing interests.

References

[1] K.S. Al-Harbi, Treatment-resistant depression: therapeutic trends, challenges, and future directions, Patient Prefer. Adherence 6 (2012) 369.
[2] B.W. Badran, K.A. Caulfield, S. Stomberg-Firestein, P.M. Summers, L.T. Dowdle, M. Savoca, X. Li, C.W. Austelle, E.B. Short, J.J. Borckardt, et al., Sonication of the anterior thalamus with MRI-guided transcranial focused ultrasound (tFUS) alters pain thresholds in healthy adults: a double-blind, sham-controlled study, Brain Stimul. 13 (2020) 1805–1812.
[3] J. Blackmore, S. Shrivastava, J. Sallet, C.R. Butler, R.O. Cleveland, Ultrasound neuromodulation: a review of results, mechanisms and safety, Ultrasound Med. Biol. 45 (2019) 1509–1536.
[4] U. Braun, A. Schaefer, R.F. Betzel, H. Tost, A. Meyer-Lindenberg, D.S. Bassett, From maps to multi-dimensional network mechanisms of mental disorders, Neuron 97 (2018) 14–31.
[5] V. Braun, J. Blackmore, R.O. Cleveland, C.R. Butler, Transcranial ultrasound stimulation in humans is associated with an auditory confound that can be effectively masked, Brain Stimul. 13 (2020) 1527–1534.
[6] A. Bystritsky, Treatment-resistant anxiety disorders, Mol. Psychiatry 11 (2006) 805–814.
[7] S.M. Chambers, C.A. Fasano, E.P. Papapetrou, M. Tomishima, M. Sadelain, L. Studer, Highly efficient neural conversion of human ES and iPS cells by dual inhibition of SMAD signaling, Nat. Biotechnol. 27 (2009) 275–280.
[8] M. Chernov, A.W. Roe, Infrared neural stimulation: a new stimulation tool for central nervous system applications, Neurophotonics 1 (2014) 011011.
[9] I. Chiaradia, M.A. Lancaster, Brain organoids for the study of human neurobiology at the interface of in vitro and in vivo, Nat. Neurosci. 23 (2020) 1496–1508.
[10] R.F. Dallapiazza, K.F. Timbie, S. Holmberg, J. Gatesman, M.B. Lopes, R.J. Price, G.W. Miller, W.J. Elias, Noninvasive neuromodulation and thalamic mapping with low-intensity focused ultrasound, J. Neurosurg. (2017) 1–10.
[11] M. Dandekar, A. Fenoy, A. Carvalho, J. Soares, J. Quevedo, Deep brain stimulation for treatment-resistant depression: an integrative review of preclinical and clinical findings and translational implications, Mol. Psychiatry 23 (2018) 1094–1112.
[12] E. Di Lullo, A.R. Kriegstein, The use of brain organoids to investigate neural development and disease, Nat. Rev. Neurosci. 18 (2017) 573–584.
[13] M. Durens, J. Nestor, M. Williams, K. Herold, R.F. Niescier, J.W. Lunden, A.W. Phillips, Y.C. Lin, D.M. Dykxhoorn, M.W. Nestor, High-throughput screening of human induced pluripotent stem cell-derived brain organoids, J. Neurosci. Methods 335 (2020) 108627.
[14] W.J. Elias, D. Huss, T. Voss, J. Loomba, M. Khaled, E. Zadicario, R.C. Frysinger, S.A. Sperling, S. Wylie, S.J. Monteith, et al., A pilot study of focused ultrasound thalamotomy for essential tremor, N. Engl. J. Med. 369 (2013) 640–648.
[15] W.J. Elias, N. Lipsman, W.G. Ondo, P. Ghanouni, Y.G. Kim, W. Lee, M. Schwartz, K. Hynynen, A.M. Lozano, B.B. Shah, et al., A randomized trial of focused ultrasound thalamotomy for essential tremor, N. Engl. J. Med. 375 (2016) 730–739.
[16] FDA, Marketing clearance of diagnostic ultrasound systems and transducers, Food and Drug Administration FDA-2017-D-5372, 2019.
[17] J.M. Ferguson, Ssri antidepressant medications: adverse effects and tolerability, Prim. Care Companion J. Clin. Psychiatry 3 (2001) 22.
[18] D. Folloni, L. Verhagen, R.B. Mars, E. Fouragnan, C. Constans, J.F. Aubry, M.F. Rushworth, J. Sallet, Manipulation of subcortical and deep cortical activity in the primate brain using transcranial focused ultrasound stimulation, Neuron 101 (2019) 1109–1116.
[19] E.F. Fouragnan, B.K. Chau, D. Folloni, N. Kolling, L. Verhagen, M. Klein-Flügge, L. Tankelevitch, G.K. Papageorgiou, J.F. Aubry, J. Sallet, et al., The macaque anterior cingulate cortex translates counterfactual choice value into actual behavioral change, Nat. Neurosci. 22 (2019) 797–808.
[20] L. Gavrilov, Focused ultrasound stimulation of the peripheral nervous system: physical basis and practical applications, Int. J. Mod. Phys., Adv. Theory Appl. 1 (2016) 45–118.
[21] M.S. George, Z. Nahas, M. Molloy, A.M. Speer, N.C. Oliver, X.B. Li, G.W. Arana, S.C. Risch, J.C. Ballenger, A controlled trial of daily left prefrontal cortex TMS for treating depression, Biol. Psychiatry 48 (2000) 962–970.
[22] N. Grossman, D. Bono, N. Dedic, S.B. Kodandaramaiah, A. Rudenko, H.J. Suk, A.M. Cassara, E. Neufeld, N. Kuster, L.H. Tsai, et al., Noninvasive deep brain stimulation via temporally interfering electric fields, Cell 169 (2017) 1029–1041.
[23] H. Guo, M. Hamilton, S.J. Offutt, C.D. Gloeckner, T. Li, Y. Kim, W. Legon, J.K. Alford, H.H. Lim, Ultrasound produces extensive brain activation via a cochlear pathway, Neuron (2018).
[24] C. Humpel, Organotypic brain slice cultures: a review, Neuroscience 305 (2015) 86–98.
[25] D.H. Jaffe, B. Rive, T.R. Denee, The humanistic and economic burden of treatment-resistant depression in Europe: a cross-sectional study, BMC Psychiatry 19 (2019) 247.
[26] S.C. Karceski, Seizure medications and their side effects, Neurology 69 (2007) E27–E29.
[27] N. Khalighinejad, A. Bongioanni, L. Verhagen, D. Folloni, D. Attali, J.F. Aubry, J. Sallet, M.F. Rushworth, A basal forebrain-cingulate circuit in macaques decides it is time to act, Neuron 105 (2020) 370–384.

[28] H. Kim, A. Chiu, S.D. Lee, K. Fischer, S.S. Yoo, Focused ultrasound-mediated non-invasive brain stimulation: examination of sonication parameters, Brain Stimul. 7 (2014) 748–756.
[29] J. Kim, B.K. Koo, J.A. Knoblich, Human organoids: model systems for human biology and medicine, Nat. Rev. Mol. Cell Biol. 21 (2020) 571–584.
[30] R.L. King, J.R. Brown, W.T. Newsome, K.B. Pauly, Effective parameters for ultrasound-induced in vivo neurostimulation, Ultrasound Med. Biol. 39 (2013) 312–331.
[31] J. Kubanek, P. Shukla, A. Das, S.A. Baccus, M.B. Goodman, Ultrasound elicits behavioral responses through mechanical effects on neurons and ion channels in a simple nervous system, J. Neurosci. (2018), 1458–17.
[32] J. Kuhn, W. Gaebel, J. Klosterkoetter, C. Woopen, Deep brain stimulation as a new therapeutic approach in therapy-resistant mental disorders: ethical aspects of investigational treatment, Eur. Arch. Psychiatry Clin. Neurosci. 259 (2009) 135–141.
[33] P.S. Larson, Deep brain stimulation for movement disorders, Neurotherapeutics 11 (2014) 465–474.
[34] P. Le Floch, Q. Li, Z. Lin, S. Zhao, R. Liu, K. Tasnim, H. Jiang, J. Liu, Stretchable mesh nanoelectronics for 3d single-cell chronic electrophysiology from developing brain organoids, Adv. Mater. 34 (2022) 2106829.
[35] W. Legon, T.F. Sato, A. Opitz, J. Mueller, A. Barbour, A. Williams, W.J. Tyler, Transcranial focused ultrasound modulates the activity of primary somatosensory cortex in humans, Nat. Neurosci. 17 (2014) 322–329.
[36] S.H. Lisanby, Electroconvulsive therapy for depression, N. Engl. J. Med. 357 (2007) 1939–1945.
[37] C.K. Loo, J.L. Taylor, S.C. Gandevia, B.N. McDarmont, P.B. Mitchell, P.S. Sachdev, Transcranial magnetic stimulation (TMS) in controlled treatment studies: are some “sham” forms active?, Biol. Psychiatry 47 (2000) 325–331.
[38] E.D. Louis, E. Rios, C. Henchcliffe, How are we doing with the treatment of essential tremor (ET)? Persistence of patients with et on medication: data from 528 patients in three settings, Eur. J. Neurol. 17 (2010) 882–884.
[39] K.E. Lyons, R. Pahwa, Deep brain stimulation and essential tremor, J. Clin. Neurophysiol. 21 (2004) 2–5.
[40] P.W. McCormick, M. Stewart, G. Lewis, M. Dujovny, J.I. Ausman, Intracerebral penetration of infrared light, J. Neurosurg. 76 (1992) 315–318.
[41] M.D. Menz, P. Ye, K. Firouzi, A. Nikoozadeh, K.B. Pauly, P. Khuri-Yakub, S.A. Baccus, Radiation force as a physical mechanism for ultrasonic neurostimulation of the ex vivo retina, J. Neurosci. 39 (2019) 6251–6264.
[42] O. Naor, S. Krupa, S. Shoham, Ultrasonic neuromodulation, J. Neural Eng. 13 (2016) 031003.
[43] H. Nemec, Interferential therapy: a new approach in physical medicine, Br. J. Physiother. 12 (1959) 9–12.
[44] Y. Nir, L. Fisch, R. Mukamel, H. Gelbard-Sagiv, A. Arieli, I. Fried, R. Malach, Coupling between neuronal firing rate, gamma LFP, and BOLD fMRI is related to interneuronal correlations, Curr. Biol. 17 (2007) 1275–1285, https://doi.org/10.1016/j.cub.2007.06.066.
[45] S.J. Oh, J.M. Lee, H.B. Kim, J. Lee, S. Han, J.Y. Bae, G.S. Hong, W. Koh, J. Kwon, E.S. Hwang, et al., Ultrasonic neuromodulation via astrocytic TRPA1, Curr. Biol. 29 (2019) 3386–3401.
[46] S.P. Paşca, Assembling human brain organoids, Science 363 (2019) 126–127.
[47] J.L. Price, W.C. Drevets, Neural circuits underlying the pathophysiology of mood disorders, Trends Cogn. Sci. 16 (2012) 61–71.
[48] G. Quadrato, T. Nguyen, E.Z. Macosko, J.L. Sherwood, S. Min Yang, D.R. Berger, N. Maria, J. Scholvin, M. Goldman, J.P. Kinney, et al., Cell diversity and network dynamics in photosensitive human brain organoids, Nature 545 (2017) 48–53.
[49] T. Riis, J. Kubanek, Effective ultrasonic stimulation in human peripheral nervous system, IEEE Trans. Biomed. Eng. (2021).
[50] T.S. Riis, T.D. Webb, J. Kubanek, Acoustic properties across the human skull, Ultrasonics 119 (2022) 106591.
[51] J.L. Sanguinetti, S. Hameroff, E.E. Smith, T. Sato, C.M. Daft, W.J. Tyler, J.J. Allen, Transcranial focused ultrasound to the right prefrontal cortex improves mood and alters functional connectivity in humans, Front. Human Neurosci. 14 (2020) 52.
[52] T. Sato, M.G. Shapiro, D.Y. Tsao, Ultrasonic neuromodulation causes widespread cortical activation via an indirect auditory mechanism, Neuron 98 (2018) 1031–1041.
[53] K.W. Scangos, G.S. Makhoul, L.P. Sugrue, E.F. Chang, A.D. Krystal, State-dependent responses to intracranial brain stimulation in a patient with depression, Nat. Med. 27 (2021) 229–231.
[54] Y. Seto, M. Eiraku, Toward the formation of neural circuits in human brain organoids, Curr. Opin. Cell Biol. 61 (2019) 86–91.
[55] T. Sharf, T. van der Molen, E. Guzman, S.M. Glasauer, G. Luna, Z. Cheng, M. Audouard, K.G. Ranasinghe, K. Kudo, S. Nagarajan, et al., Intrinsic network activity in human brain organoids, 2021, available at SSRN 3797268.
[56] J. Sidhaye, J.A. Knoblich, Brain organoids: an ensemble of bioassays to investigate human neurodevelopment and disease, Cell Death Differ. 28 (2021) 52–67.
[57] K. Tasnim, J. Liu, Emerging bioelectronics for brain organoid electrophysiology, J. Mol. Biol. 434 (2022) 167165.
[58] G. Thut, A. Pascual-Leone, A review of combined TMS-EEG studies to characterize lasting effects of repetitive TMS and assess their usefulness in cognitive and clinical neuroscience, Brain Topogr. 22 (2010) 219.
[59] V. Velling, S. Shklyaruk, Modulation of the functional state of the brain with the aid of focused ultrasonic action, Neurosci. Behav. Physiol. 18 (1988) 369–375.
[60] L. Verhagen, C. Gallea, D. Folloni, C. Constans, D.E. Jensen, H. Ahnine, L. Roumazeilles, M. Santin, B. Ahmed, S. Lehéricy, et al., Offline impact of transcranial focused ultrasound on cortical activation in primates, eLife 8 (2019) e40541.
[61] Y. Wang, S. Chiola, G. Yang, C. Russell, C.J. Armstrong, Y. Wu, J. Spampanato, P. Tarboton, H.A. Ullah, N.U. Edgar, et al., Modeling human telencephalic development and autism-associated SHANK3 deficiency using organoids generated from single neural rosettes, Nat. Commun. 13 (2022) 5688.
[62] A.S. Widge, D.D. Dougherty, Deep brain stimulation for treatment-refractory mood and obsessive-compulsive disorders, Curr. Behav. Neurosci. Rep. 2 (2015) 187–197.
[63] P.P. Ye, J.R. Brown, K.B. Pauly, Frequency dependence of ultrasound neurostimulation in the mouse brain, Ultrasound Med. Biol. 42 (2016) 1512–1530.
[64] T.A. Zesiewicz, A. Chari, I. Jahan, A.M. Miller, K.L. Sullivan, Overview of essential tremor, Neuropsychiatr. Dis. Treat. 6 (2010) 401.